

# Illumination Model for Two-layer Thin Film Structures

Fukun Wu<sup>1,2</sup> and Changwen Zheng<sup>1</sup>

<sup>1</sup>*Science and Technology on Integrated Information System Laboratory, Institute of Software,  
Chinese Academy of Sciences, Beijing, China*

<sup>2</sup>*University of Chinese Academy of Sciences, Beijing, China*

**Keywords:** Interference Effects, Multilayer Film Interference Method, Fresnel Coefficients, Microfacet Factor.

**Abstract:** To address the problem of visualizing the interference effects of objects with multilayer film structures such as soap bubbles, optical lenses and Morpho butterflies in the physics-based framework, a novel full-spectrum multilayer film interference method is presented. This method applies the multi-beam interference equation to effectively simulate the multiple reflection and transmission inside films, and calculate the composite reflectance and transmittance to model the amplitude and phase variations related to interference. The Fresnel coefficients used for metallic and dielectric films are introduced to explain the absorption of photons due to the film materials, and the microfacet scattering factor is also applied to simulate the complex optical effects such as the isotropic and anisotropic phenomena caused by the roughness of the surface geometry. This method is integrated into the existing ray tracer to further enhance the photorealistically rendering capabilities. The experimental results demonstrate that our method can efficiently model the phase and amplitude information of wave to generate high-quality realistic interference effects.

## 1 INTRODUCTION

Photorealistic rendering is the main rendering technology of the existing modeling softwares such as Maya, 3Dmax and Blender. Different from the non-photorealistic rendering technology, it is involved in the physical simulation of interaction between light and objects where the illumination information can be accurately modeled. The ray tracing is generally used for modeling the propagation process of light in space. Specially, it calculate the reflectivity and transmissivity from surfaces by acquiring the material properties of objects, and eventually obtains the radiant energy of each ray arriving at the imaging plane after recursively tracing rays to generate the realistic images.

The thin film interference is an important part of photorealistically rendering. However, the existing graphical development platform or softwares lack the ability of describing the phase of light. To construct precise interference model to model the interaction between light and multilayer film structures in order to visualize iridescent colors of objects coated with multilayer films such as soap bubble, beetles and butterflies is a significant but challenging research task. In computer graphics, many wave models have been developed to render the wave phenomena gen-

erated by these multilayer film structures. Gondek et al. (Gondek et al., 1994), for example, used a wavelength-dependent bidirectional reflectance distribution function and a virtual goniospectrophotometer to analyze and generate the reflection spectrum of thin films and pearl materials. Hirayama et al. (Hirayama et al., 1999; Hirayama et al., 2000) constructed a series of multilayer dielectric and metallic film models to visualize the richer interference effects through the iterative calculation of multi-beam reflection and transmission. Sun (Sun, 2006) applied the analytical calculation and the numerical simulation methods to implement an iridescent shading process to render the biological iridescences. These method can approximately describe the wave properties of films, but rarely consider the microstructure or material characteristics of surfaces, which not applicable for the accurate simulation of the anisotropic iridescent colors.

For the sake of accurately rendering the optical phenomena of diverse film materials, this paper constructs a general multilayer film interference shader in the ray-based framework. It adopts the multi-beam interference equation and Fresnel formulae to account for the multiple reflection, interference and absorption of light. Fresnel coefficients for dielectric and metallic films are introduced to visualize interference

due to the complex refractive indexes. In addition, the irregularity of multilayer film microstructures is incorporated into the iridescent illumination model to accurately describe the isotropic and anisotropic optical properties. The new wave bidirectional scattering distribution function is proposed and integrated into the PBRT (Pharr and Humphreys, 2010) in the form of the material plugin, which has become a practical technology by applying the existing modeling software to render complex interference optical effects.

## 2 RELATED WORK

In computer graphics, to solve the problem of wave rendering in the physics-based rendering framework, multiple classical technologies have been developed where the wave scattering model is applied to simulate the behavior of light on surfaces (Smits and Meyer, 1990; Dias, 1991; Gondek et al., 1994; Callet, 1996; Dumazet and Callet, 2009; Jakob et al., 2014). For instance, Moravec (Moravec, 1981) used the wave theory of light to solve the global illumination problem and applied wave model to computer graphics based on the phase tracking technology. Kajiya (Kajiya, 1986) developed a bidirectional reflectance distribution function to model the anisotropic spectral reflectance by numerically calculating Kirchhoff integral. Later, Stam (Stam, 1999) implemented a general diffraction shaders, followed by the works of Agu (Agu, 2002), Sun (Sun et al., 2000) and Wu (Wu and Zheng, 2013), to render iridescent colors from periodic structures such as compact discs in a ray-based renderer. The solutions above, however, are constructed to model diffraction effects that are a part of wave rendering, not applicable for rendering film interference effects due to the lack of ability of encapsulating phase variations into transmitted radiant energy.

To construct the accurate interference model to model the interactive behavior of light and surfaces in order to visualize the iridescent appearance of objects coated with multilayer films such as soap bubble, beetles and butterflies has attracted a lot of attentions. There exist many models used for rendering these interference effects generated by multilayer films. Icart et al. (Icart and Arquès, 2000), for example, constructed a physics-based bidirectional reflectance model for multilayer systems consisting of homogeneous and isotropic thin films with rough boundaries, which can account for interference, diffraction and polarization effects. Hirayama et al. (Hirayama et al., 1999; Hirayama et al., 2000; Hirayama et al., 2001) constructed a comprehensive multilayer film inter-

ference model to model scattering characteristics of rough multilayer surfaces. Sun (Sun, 2006) implemented an iridescent shading process for rendering the biological iridescences of butterflies and beetles due to multilayer interference based on analytical calculation and numerical simulation. Few of the previous models, however, takes into account specific geometrical properties of multilayer films or other sub-wavelength microstructures. They also lack the ability of modeling the back-scattering and anisotropic properties for photorealistic renderings of Morpho butterfly. Okada et al. (Okada et al., 2013) applied the nonstandard finite-difference time-domain method to numerically solve Maxwell's equations for brilliant iridescences. This approach can gain accurate results, but depends on a fine defined numerical grid. Hill et al. (Hill et al., 2014) made a comprehensive description of physically based shading approaches which is used as the basis of our proposed model.

## 3 IRIDESCENT ILLUMINATION MODEL

The key to rendering iridescent colors of multilayer films in the ray-based framework is to account for the interaction between the films with the periodic structure and light with amplitude and phase. Therefore, this paper builds on the multilayer film interference theory and incorporates the geometry of rough surfaces to construct an accurate film interference shader in order to model isotropic and anisotropic iridescent effects, which is further integrated in Maya modeling software to improve its practicality. The iridescent colors from objects coated with similar multilayer films can be efficiently visualized where the refractive indexes, thicknesses and amount of alternative arrangement of films and the incident direction of light source play an important role.

### 3.1 Multi-beam Interference

When light interacts with multilayer films, it undergoes multiple reflection, transmission and absorption inside films. It is desired to develop a more general model that take complex interactions into consideration. In this work, we analytically compute multilayer film interference based on the recursive composition method (Hirayama et al., 1999; Sun, 2006) to visualize optical properties of multilayer structures.

As an example, consider a pair of film and air layers as shown in Figure 1. Given a thickness  $H$  and a refractive index  $n_j, j = 0, 1, 2$ . The  $r_1, r_2, t_1$  and  $t_2$  denote the reflection and transmission coefficients

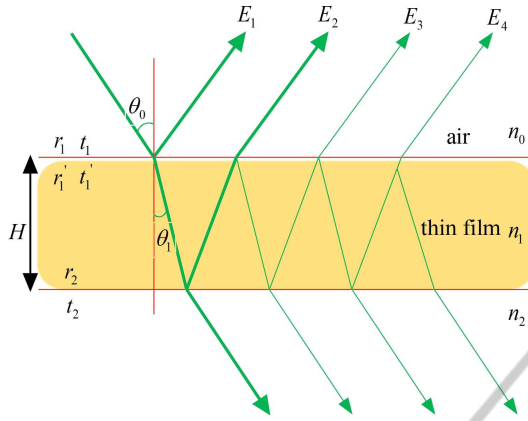


Figure 1: Interference modeling from a single layer film structure of ridge.

of light propagating from air to film, and the  $r_1'$  and  $t_1'$  denote the reflection and transmission coefficients of light propagating from film to air, which are derived using the Fresnel equations. The refractive angle complies with Snell's law. The indices of refraction of the air and the film are denoted as  $n_0$  and  $n_1$  respectively where  $n_0 = n_2$ .

Hence the reflectivity of light from a pair of film and air layers corresponding to Figure 1 are formulated as

$$\begin{aligned} E_1^{(r)} &= r_1 E_0^{(r)} \\ E_2^{(r)} &= t_1 r_2 t_1' E_0^{(r)} e^{i\delta} \\ E_3^{(r)} &= t_1 r_2 (r_1' r_2) t_1' E_0^{(r)} e^{i2\delta} \\ E_4^{(r)} &= t_1 r_2 (r_1' r_2)^2 t_1' E_0^{(r)} e^{i3\delta} \\ &\vdots \end{aligned} \quad (1)$$

where  $\delta = \frac{4\pi}{\lambda} n_1 H \cos\theta_1$  denotes the phase difference of two adjacent reflected or transmitted light propagating through the film.

Referring to the interference theory of multilayer films (Born and Wolf, 2005; Goodman, 2005; Liang, 2008; Hirayama et al., 1999), the composite reflectivity  $\bar{r}$  and transmissivity  $\bar{t}$  of this single layer film can be further formulated as

$$\bar{r} = \frac{E_1^{(r)} + E_2^{(r)} + \dots}{E_0^{(r)}} \approx \frac{r_1 + r_2 e^{i\delta}}{1 + r_1 r_2 e^{i\delta}} \quad (2)$$

Similarly, the transmitted coefficient is given by

$$\bar{t} \approx \frac{t_1 + t_2}{1 + r_1 r_2 e^{i\delta}} \quad (3)$$

For two or more M-layer thin film system, we can iterative the calculation of the reflection and transmission coefficients from the last layer adjacent to the

substrate to the first layer. For the Mth layer, for instance,

$$\bar{r}_M = \frac{r_M + r_{M+1} e^{i\delta_M}}{1 + r_M r_{M+1} e^{i\delta_M}} \quad (4)$$

$$\bar{t}_M = \frac{t_M t_{M+1}}{1 + r_M r_{M+1} e^{i\delta_M}} \quad (5)$$

where  $\delta$  is defined as

$$\delta_M = \frac{4\pi}{\lambda} n_M H_M \cos\theta_M \quad (6)$$

The calculation process is repeated until the first layer adjacent to air. Finally, we can obtain the composite reflectivity and transmissivity coefficients of the multilayer film system.

Taking the above single layer film for example and ignoring the polarization of the light, we can get the reflectance distribution function of the film, namely,

$$R_{fresnel} = \frac{r_1^2 + r_2^2 + 2r_1 r_2 \cos\delta}{1 + r_1^2 r_2^2 + 2r_1 r_2 \cos\delta} \quad (7)$$

The transmittance distribution derivation of the film is written as

$$T_{fresnel} = \frac{n_2 \cos\theta_1}{n_0 \cos\theta_0} \frac{t_1^2 t_2^2}{1 + r_1^2 r_2^2 + 2r_1 r_2 \cos\delta} \quad (8)$$

The thin film interference is one of most simple structural colors and widely exists in nature. Its most remarkable characteristics is that the reflected wave is selective. Namely, a specific wavelength plays a determinant role in a specific direction. Based on the Equation 7, the construction interference condition of reflected wave is given by

$$2n_1 H \cos\theta_1 = m\lambda \quad (9)$$

Referring to the above constructive equation, it is clear that the wavelength leading to higher reflectivity changes to a shorter wavelength with the increase of the incident angle. The result is that the color changes with viewing angle. For example, the color of Morpho butterflies changes from blue to purple as the viewing angle is increased that will be verified in the following experiment.

### 3.2 Fresnel Coefficient

According to the above section, the composite reflection and transmission coefficients on film surfaces play a key role in producing iridescent colors. They affect the spatial distribution of radiant energy by changing the amplitude and phase of light, which are determined by Fresnel equation 10. In experiments, light is assumed to be unpolarized and randomly oriented. Hence, the reflectance of multilayer film structure is approximated as the average of squares of the parallel and perpendicular polarization Fresnel terms.

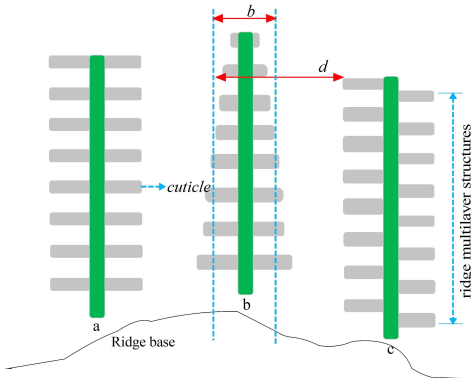


Figure 2: The approximated geometry of ridge films where the film width  $b$  is set to 300 nm and the film separation  $d$  is set to 675 nm based on the measurements of Platter (Platter, 2004).

$$\begin{aligned}
 r_j^{\parallel} &= \frac{n_j \cos \theta_{j-1} - n_{j-1} \cos \theta_j}{n_j \cos \theta_{j-1} + n_{j-1} \cos \theta_j} \\
 t_j^{\parallel} &= \frac{2n_{j-1} \cos \theta_{j-1}}{n_{j-1} \cos \theta_j + n_j \cos \theta_{j-1}} \\
 r_j^{\perp} &= \frac{n_{j-1} \cos \theta_{j-1} - n_j \cos \theta_j}{n_{j-1} \cos \theta_{j-1} + n_j \cos \theta_j} \\
 t_j^{\perp} &= \frac{2n_{j-1} \cos \theta_{j-1}}{n_j \cos \theta_j + n_{j-1} \cos \theta_{j-1}}
 \end{aligned} \quad (10)$$

where  $r^{\parallel}$  and  $r^{\perp}$  denote the Fresnel coefficients for parallel polarized light,  $t^{\parallel}$  and  $t^{\perp}$  denote the coefficients for perpendicular polarized light, and  $n_{j-1}$  and  $n_j$  denote the refractive indexes of incident and transmitted medium respectively. The transmitted angle complies with Snell's law (Hirayama et al., 1999; Pharr and Humphreys, 2010).

The applied Fresnel term, namely Equation 10, depends on the assumption that the potential polarization states of the light are not considered. This is an approximation, as the reflected parallel term can lead to a phase shift, or, in the case of total reflection, become purely imaginary, therefore leading again to a phase delay. On the other hand, the perpendicular Fresnel term does not affect the phase. These situations, which may be important for interference, are neglected by averaging them.

### 3.3 Regularity and Irregularity of Structures

For the multilayer film structures with a certain amount of irregularity such as Morpho butterflies, the occlusion, shadowing and interreflection of light among ridges may lead to the uneven spatial distribution of energy as illustrated in Figure 2. For example,

Kinoshita and Yoshioka (Kinoshita et al., 2002; Kinoshita and Yoshioka, 2005) have demonstrated that the behavior of light is the result of joint action of the regularity and irregularity of multilayer film structures.

It is necessary to incorporate the irregularity of the film structure to model the diffusive nature where isotropic Phong exponent (Phong, 1975) is commonly used (Sun, 2006). However, some film structures often show backscattering and anisotropic spectral characteristics. Many geometrical models have been developed (Torrance and Sparrow, 1967; Blinn, 1977; Wu et al., 2010). They work by statistically modeling the scattering of light, where the wave-like properties are ignored. As an extension, we incorporate the Ashikhmin microfacet scattering shader (Ashikhmin and Shirley, 2000), namely Equation 11, into the wave BSDF illumination model to describe the local anisotropic effects.

$$D_{facet} = \frac{\sqrt{(e_x + 2)(e_y + 2)}}{2\pi} (\omega_h \cdot n)^{e_x \cos^2 \phi + e_y \sin^2 \phi} \quad (11)$$

where  $\omega_h$  denotes the half angle vector for incident direction  $\omega_i$  and outgoing direction  $\omega_o$ ,  $n$  denotes the surface normal,  $\phi$  denotes the orientation angle, and  $e_x$  and  $e_y$  denote the exponents of anisotropic distribution along the x and y axes respectively.

This paper develops a new wave bidirectional scattering distribution function that provides an efficient way in accurately rendering the interference appearance of films with periodic structures, written as

$$\text{BSDF}_{\lambda} = c_a I_{diffuse} + c_b \frac{D_{facet} F_{fresnel} G(\omega_o, \omega_i)}{4 \cos \theta_o \cos \theta_i} \quad (12)$$

where  $I_{diffuse}$  denotes the diffuse effects due to the surface irregularities,  $F_{fresnel}$  is determined by Equations 7 and 8, and  $c_a$  and  $c_b$  is the weighted coefficient. A geometric attenuation term  $G(\omega_o, \omega_i)$  is defined as (Torrance and Sparrow, 1967; Pharr and Humphreys, 2010)

$$G(\omega_o, \omega_i) = \min\left(1, \frac{2(n \cdot \omega_h)(n \cdot \omega_o)}{\omega_o \cdot \omega_h}, \frac{2(n \cdot \omega_h)(n \cdot \omega_i)}{\omega_o \cdot \omega_h}\right) \quad (13)$$

where  $\omega_h$  denotes the bisector of  $\omega_i$  and  $\omega_o$ , and  $n$  is the surface normal.

## 4 SIMULATIONS

We implemented our wave model for rendering iridescent colors of objects coated with multilayer thin

films by creating a new material plugin for the PBRT system (Pharr and Humphreys, 2010). All of the images in this work were produced using Maya software on a Dell T7600 workstation with a 2.40 GHz Intel Xeon CPU E5-2609 and a NVIDIA Quadro 6000. We focused on the visible spectrum (350~750 nm) and showed physics-based renderings as interference examples for the multilayer structures.

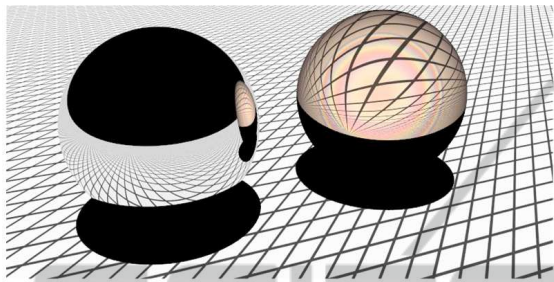


Figure 3: Renderings from a mirror sphere with perfect specular reflection (left) and a glass sphere coated with the 420 nm dielectric film (right).

Figure 3 visualizes the optical phenomena of a single layer dielectric film coating on a glass sphere due to the multi-beam interference where refractive indices of the glass and dielectric materials are set to 1.5 and 2.0 respectively. Note how refraction through the transmissive object distorts the scene behind it and how the left mirror reflects the interference effect.

In Figure 4, our model is further applied to render the iridescent patterns of objects coated with a 450 nm dielectric film, whose interference effects clearly appear on the near mirror surface. The indices of refraction of substrate and dielectric are set to 1.5 and 2.0. Compared with Figure 3, the color shows a shift to red with the increase of the film thickness which is in agreement with the experiments.

This paper also implements the film interference patterns of opaque objects as illustrated in Figure 5 where Blinn (Blinn, 1977) isotropic exponent is used. The indices of refraction of substrate and dielectric are also set to 1.5 and 2.0. In addition, the approach proposed in this article is applicable for other cases of iridescence rendering. For example, Figures 6 and 7 are two examples of anisotropic renderings of opaque objects based on the proposed approach in the physics-based PBRT (Pharr and Humphreys, 2010), where the parameters denoting the film thickness and the microfacet roughness used for each object can be easily adjusted as needed. We addressed the effects of the surface roughness and anisotropy on the visual optical appearance where Ashikhmin (Ashikhmin and Shirley, 2000) anisotropic functions is used as the basis.

The iridescent objects can be biological or nonbio-

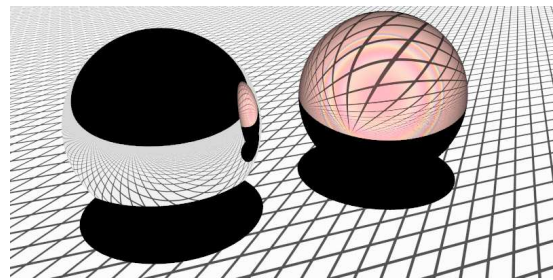


Figure 4: Renderings from a mirror sphere coated with perfect specular reflection (left) and a glass sphere with the 450 nm dielectric film (right).

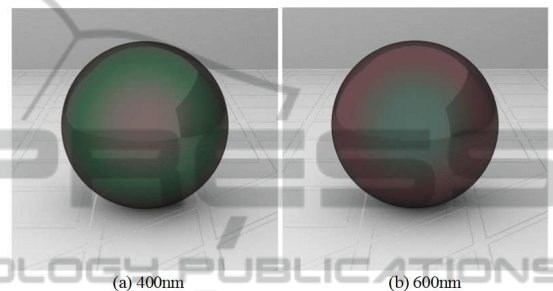


Figure 5: Interference renderings of opaque objects coated with 400 nm and 600 nm dielectric films respectively.

logical. With the help of the optics and electric microscopes, researchers have extensively reported the tree-like periodic structures of ridges on Morpho butterfly wings as shown in Figure 2 where ridges consist of alternate cuticle film and air. Our proposed model can be used for generate iridescent colors of butterflies as illustrated in Figure 8. The four butterflies with different structural parameter values are rendered, where the thickness of film layer is set to 80 nm, 100 nm, 120 nm, and 135 nm respectively. From left to right, the rendered colors of wings are approximate violet, blue, yellow and red. Comparing these cases, a color shift from the violet to the red happens. A detailed comparison with the work of Sun (Sun, 2006) is further illustrated in Figure 9. This renderings also agree with the observed iridescences and experimental measurements of Morpho butterflies (Fox, 1976; Simon, 1971; Vukusic et al., 1999). This experimental measurements provide us with a basis to apply the multilayer interference model to visualize the iridescent colors reflected by the biological structures.

## 5 CONCLUSION AND FUTURE WORK

In the photorealistic rendering field, a lot of attentions are paid to the wave properties of

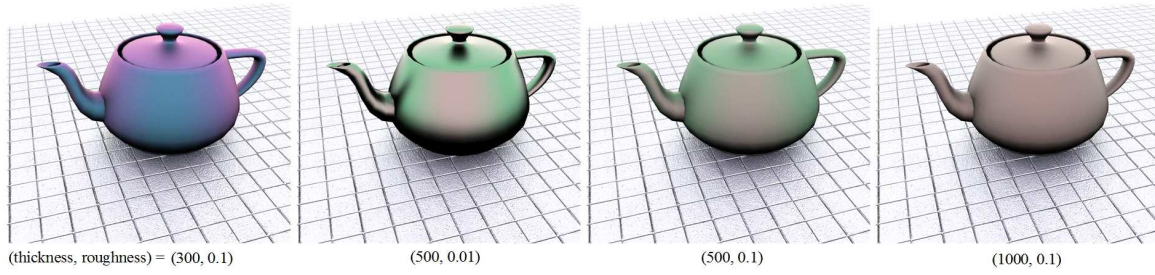


Figure 6: Interference renderings of teapots with the different surface roughnesses and thin film thicknesses.

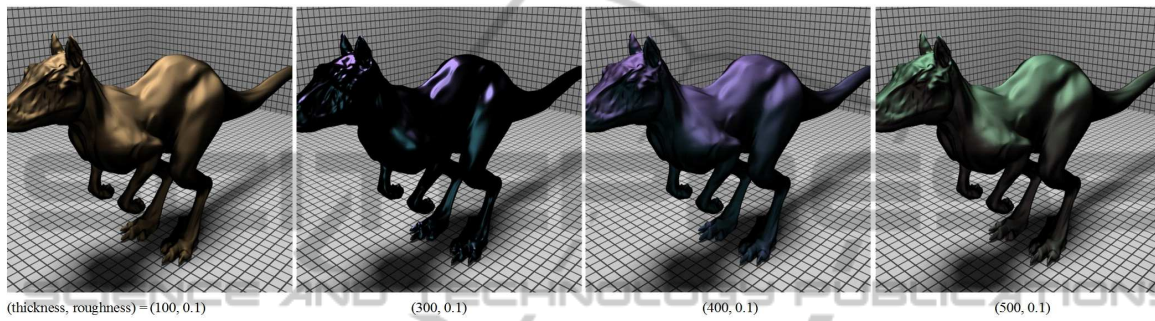


Figure 7: Interference renderings of kangaroos with the different surface roughnesses and thin film thicknesses.

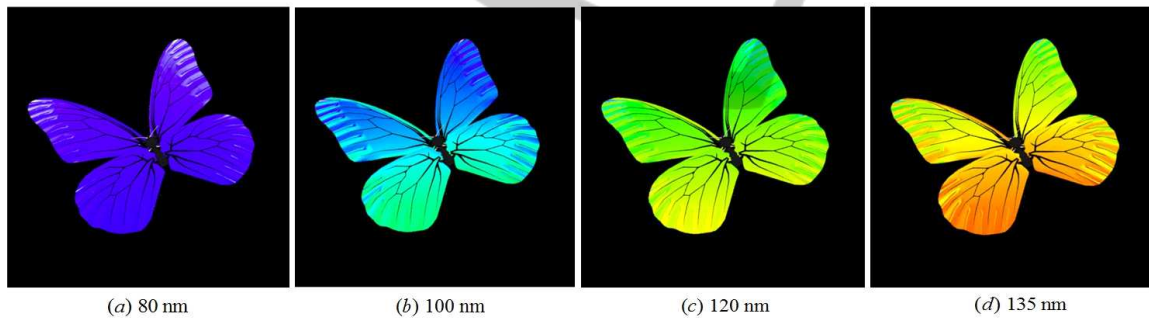


Figure 8: Rendered biological iridescences of Morpho butterflies consisting of tree-like ridge structures with cuticle films of different thicknesses (left to right: 80 nm, 100 nm, 120 nm and 135 nm).

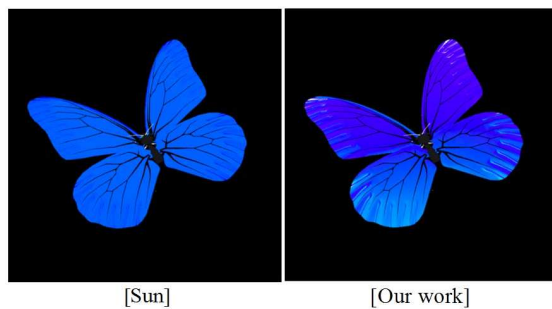


Figure 9: Comparison of rendered biological iridescences of Morpho butterfly wings with 90nm cuticle layer thickness using Sun butterfly shader (Sun, 2006) (left) and our proposed multilayer interference model (right) respectively.

multilayer film structures. This paper constructs an interference illumination model to visualize the iridescent colors caused by the interaction of light and layered structures where the indices of refraction, thicknesses and the irregular geometry of films play an important role. In ray tracers, This model creates a wavelength-dependent bidirectional scattering distribution function to describe the spatial spectrum distribution of light. The multi-beam interference equations have been introduced to represent the multiple reflection and transmission inside films in order to realistically render local illumination. The Fresnel formulae for dielectric and metallic films are also described which are applied to trace the amplitude and phase variations. In addition, the microfacet scattering coefficient is incorporated to consider

the optical characteristics from rough surfaces for the sake of accurately exhibiting backscattering and anisotropic phenomena. Compared with experimental measurements, we have shown that this model suffices to describe the optical effects, and have facilitated its practical application in Maya software.

However, there still exist lots of work for future. For example, how to handle the polarized effects of light. Due to the complexity of film structures, it is desirable to gain the measured appearance data to improve accuracy of wave rendering. It may also be necessary to consider the special anti-aliasing such as spectral ray differential (Elek et al., 2014) in order to addressing the issue of high frequencies in the spectrum. In addition, our proposed model can be applied to render other objects exhibiting structural colors such as optical lenses, beetles and birds.

## ACKNOWLEDGEMENTS

We sincerely acknowledge all anonymous reviewers for their valuable comments. This work was funded by National High Technology Research and Development Program of China (2012AA011206 and 2009AA01Z303).

## REFERENCES

- Agu, E. (2002). Diffraction shading models for iridescent surfaces. In *Proceedings of IASTED VIII*.
- Ashikhmin, M. and Shirley, P. (2000). An anisotropic phong brdf model. *Journal of Graphics Tools*, 5(2):25–32.
- Blinn, J. (1977). Models of light reflection for computer synthesized pictures. In *Proceedings of SIGGRAPH '77*, pages 192–198.
- Born, M. and Wolf, E. (2005). *Principles of Optics: Electromagnetic Theory of Propagation, Interference and Diffraction of Light*. Cambridge University Press, 7th edition.
- Callet, P. (1996). Pertinent data for modelling pigmented materials in realistic rendering. *Computer Graphics Forum*, 15(2):119–127.
- Dias, M. (1991). Ray tracing interference color. *IEEE Computer Graphics and Applications*, 11(2):54–60.
- Dumazet, S. and Callet, P. (2009). Simulation of pearls, physically based rendering, the virtuelium approach. In *AIC Congress, Sydney, Australia*.
- Elek, O., Bauszat, P., Ritschel, T., Magnor, M., and Seidel, H.-P. (2014). Spectral ray differentials. *Computer Graphics Forum (Proceedings of EGSR)*, 33(4).
- Fox, D. (1976). *Animal Biochromes and Structural colours*. University of California Press, Berkeley, CA.
- Gondek, J., Meyer, G., and Newman, J. (1994). Wavelength dependent reflectance functions. In *Proceedings of SIGGRAPH '94*, pages 213–219.
- Goodman, J. (2005). *Introduction to Fourier optics*. Roberts&Co., Englewood, Colo., 3rd edition.
- Hill, S., McAuley, S., Dupuy, J., Gotanda, Y., Heitz, E., Hoffman, N., Lagarde, S., Langlands, A., Megibben, I., Rayani, F., and de Rousiers, C. (2014). Physically based shading in theory and practice. In *ACM SIGGRAPH 2014 Courses*, SIGGRAPH '14, pages 23:1–23:8, New York, NY, USA. ACM.
- Hirayama, H., Kaneda, K., Yamashita, H., and Monden, Y. (2001). An accurate illumination model for objects coated with multilayer films. *Computers & Graphics*, 25(3):391–400.
- Hirayama, H., Kaneda, K., Yamashita, H., Monden, Y., and Yamaji, Y. (1999). Visualization of optical phenomena caused by multilayer films with complex refractive indices. In *Proceedings of the 7th Pacific Conference on Computer Graphics and Application*, pages 128–137.
- Hirayama, H., Yamaji, Y., Kaneda, K., Yamashita, H., and Monden, Y. (2000). Rendering iridescent colors appearing on natural objects. In *Proceedings of the 8th Pacific Conference on Computer Graphics and Application*, pages 15–22.
- Icart, I. and Arquès, D. (2000). A physically-based brdf model for multilayer systems with uncorrelated rough boundaries. In *Rendering Techniques*, pages 353–364.
- Jakob, W., D'Eon, E., Jakob, O., and Marschner, S. (2014). A comprehensive framework for rendering layered materials. In *Proceedings of SIGGRAPH '14*.
- Kajiya, J. (1986). The rendering equations. In *Proceedings of SIGGRAPH '86*, volume 20, pages 143–150.
- Kinoshita, S. and Yoshioka, S. (2005). Structural colors in nature: the role of regularity and irregularity in the structure. In *ChemPhysChem*, volume 6, pages 1442–1459.
- Kinoshita, S., Yoshioka, S., Fujii, Y., and Okamoto, N. (2002). Photophysics of structural color in the morpho butterflies. In *Forma*, volume 17, pages 103–121.
- Liang, Q. (2008). *Physical optics*. Publishing House of Electronics Industry, 3rd edition.
- Moravec, H. (1981). 3d graphics and the wave theory. In *Proceedings of SIGGRAPH '81*, pages 289–296.
- Okada, N., Zhu, D., Cai, D., Cole, J., Kambe, M., and Kinoshita, S. (2013). Rendering morpho butterflies based on high accuracy nano-optical simulation. *Journal of Optics*, 42(1):25–36.
- Pharr, M. and Humphreys, G. (2010). *Physically based rendering: from theory to implementation*. Morgan Kaufmann, 2nd edition.
- Phong, B. (1975). Illumination for computer generated pictures. *Communications of the ACM*, 18(6):311–317.
- Plattner, L. (2004). Optical properties of the scales of morpho rhetenor butterflies: theoretical and experimental investigation of the back-scattering of light in the visible spectrum. *Computer Graphics Forum*, 1:49–59.
- Simon, H. (1971). *The Splendor of Iridescence of Structural Colors in the Animal World*. Dodd, Mead & Company, New York, NY.

- Smits, B. and Meyer, G. (1990). Newton's colors:simulating interference phenomena in realistic image synthesis. In *Proceedings of Eurographics Workshop on Photosimulation, Realism and Physics in Computer Graphics*, pages 185–194.
- Stam, J. (1999). Diffraction shaders. In *Proceedings of SIGGRAPH '99*, pages 101–110.
- Sun, Y. (2006). Rendering biological iridescences with rgb-based renderers. *ACM Transactions on Graphics*, 25(1):100–129.
- Sun, Y., Fracchia, F., Drew, M., and Calvert, T. (2000). Rendering iridescent colors of optical disks. In *EGWR*, pages 341–352.
- Torrance, K. and Sparrow, E. M. (1967). Theory of off-specular reflection from roughened surfaces. *Journal of the Optical Society of America*, 57(9):1105–1112.
- Vukusic, P., Sambles, J., Lawrence, C., and Wootton, R. (1999). Quantified interference and diffraction in single morpho butterfly scales. In *Proceedings of the Royal Society B:Biological Sciences*, volume 266, pages 1403–1411.
- Wu, F.-K. and Zheng, C.-W. (2013). A comprehensive geometrical optics application for wave rendering. *Graphical Models*, 75(6):318–327.
- Wu, J.-Z., Zheng, C.-W., and Hu, X.-H. (2010). Realistic rendering of bokeh effect based on optical aberrations. *The Visual Computer*, 26:555–563.